Photosynth Res (2008) 96:83–97
DOI 10.1007/s11120-007-9287-5

REGULAR PAPER

Analysis of initial chlorophyll fluorescence induction kinetics in chloroplasts in terms of rate constants of donor side quenching release and electron trapping in photosystem II

Wim J. Vredenberg

Received: 18 July 2007 / Accepted: 21 December 2007 / Published online: 15 January 2008

Abstract The fluorescence induction $F(t)$ of dark-adapted chloroplasts has been studied in multi-turnover 1 s light flashes (MTFs). A theoretical expression for the initial fluorescence rise is derived from a set of rate equations that describes the sequence of transfer steps associated with the reduction of the primary quinone acceptor Q_A and the release of photochemical fluorescence quenching of photosystem II (PSII). The initial $F(t)$ rise in the hundreds of μs time range is shown to follow the theoretical function dictated by the rate constants of light excitation (k_L) and release of donor side quenching (k_{si}). The bi-exponential function shows sigmoidicity when one of the two rate constants differs by less than one order of magnitude from the other. It is shown, in agreement with the theory, that the sigmoidicity of the fluorescence rise is variable with light intensity and mainly, if not exclusively, determined by the ratio between rate of light excitation and the rate constant of donor side quenching release.

Keywords Photosystem II · Chlorophyll fluorescence induction · Donor side quenching · Sigmoidicity · Intersystem energy transfer

Abbreviations

$B(t)$	Normalized area above rFv(t)
DCMU	3(3,4-Dichlorophenyl)-1,1-dimethylurea
DSQ	Donor side quenching
$Fm^{S(M)TF}$	Fluorescence level of system with 100% closed PSUs after S(M)TF excitation in dark-adapted state
Fo	Fluorescence level of system with 100% open PSUs in dark-adapted state
rFv	Relative variable fluorescence $(F - Fo)/(Fm - Fo)$
k_{-1}	Rate constant of radical pair recombination
k_{AB}	Rate constant of Q_A^- oxidation
k_d	Rate constant of non-radiative radical pair transfer
k_e	Rate constant of Q_A photoreduction (charge stabilization at acceptor side)
k_L	Excitation rate of photosystem in light pulse
k_t	Rate constant of photochemical trapping (charge separation) in PSII
k_w	Rate constant of non-photochemical energy losses
$k_{yi,si}$	Rate constant of P^+- and Y_Z^+-reduction, respectively, fo′r OEC in $S = S_i$-state ($i = 0, \ldots, 3$)
nFv	Normalized variable fluorescence $(F - Fo)/Fo$
q	Fraction of RCs with Q_A^-
q^{dsq}	Fraction of RCs in which acceptor- and donor side quenching is released
MTF	Multi-turnover flash (light pulse)
OEC	Oxygen evolving complex
ODE	Ordinary linear differential equation
Φ_{tr}^o	Electron trapping efficiency of open RCs
P680 (or P)	Mainstream electron donor of PSII
Phe (or Ph)	Pheophytin, primary electron acceptor of PSII
PSII	Photosystem II
PSU II	Photosynthetic unit of PSII

W. J. Vredenberg (✉)
Department of Plant Physiology, Wageningen University and Research (WUR), Arboretumlaan 4, 6703 BD Wageningen, The Netherlands
e-mail: wim.vredenberg@wur.nl

Q_A	Primary quinone acceptor of PSII
Q_B	Secondary quinone acceptor of PSII
RCII	Reaction center of PSII
STF	Single turnover flash (excitation)
TSTM	Three-state trapping model
Y_Z	Secondary electron donor of PSII

Introduction

Monitoring of chlorophyll (Chl) *a* fluorescence kinetics of photosystem II (PSII) provides a powerful experimental means to study the mechanism and dynamics of the primary and secondary photosynthetic events on a time scale ranging from nanoseconds to tens of seconds. Chl fluorescence yield in vivo and in chloroplasts changes substantially with time upon actinic illumination. Since its first clear understanding (Duysens and Sweers 1963), the variable fluorescence $F(t)$ of PSII has been the subject of many reviews (see various chapters in Govindjee et al. 1986; Papageorgiou and Govindjee 2004; Krause and Weiss 1991; Dau 1994; Lazár 2006). Several models have been presented which quantitatively relate the increase in fluorescence with the decrease in the efficiency of photochemical energy conversion in the photosynthetic reaction centers (RC) due to their closure. Closure of a RC finishes its capability for energy trapping (Vredenberg and Duysens 1963). In PSII, the light-driven reduction of the primary quinone electron acceptor (Q_A) is considered to reflect the closure of the RCII; this reduction is thought to release the quenching properties of Q_A. Fluorescence changes elicited with (sub-)ns excitations have indicated that the oxidized donor of PSII ($P680^+$) quenches the fluorescence as well (Butler 1972; Mauzerall 1972). The basics and the early history of Chl fluorescence have been reviewed by Govindjee (2004).

The time pattern of the light-induced change in fluorescence emission, is known as the fluorescence induction curve $F(t)$ (Govindjee and Papageorgiou 1971; Briantais et al. 1986). In general, it shows a multiphasic rise in a high intensity multiturnover light pulse (MTF) from the initial low dark fluorescence level Fo due to full photochemical quenching in so-called open centers toward a 5–7 times higher quasi-stationary maximal level Fm(= Fm^{MTF}) when all centers have become closed. A nomenclature has been introduced (Schreiber and Neubauer 1987; Strasser and Govindjee 1992; Strasser et al. 1995) for the $F(t)$ rise from Fo at level O to Fm at level P via two intermediate levels J and I. The fluorescence rise $F(t)$ has been denoted either as O–I_1–I_2–M (Schreiber and Neubauer 1987) or O–J–I–P (Strasser et al. 1995). The subsequent inflection points in the curve associated with the J-, I-, and P-levels in multi-turnover light pulses (MTFs) are at about 2, 100, and 500 ms. At high intensity MTFs, the kinetic pattern in the 0.01–20 ms time range shows a clear dip D at 2 ms and a substantial shift of the J-level towards 0.5–0.8 ms (Schansker et al. 2006). Under stress conditions associated with donor side inhibition (heat, drought, chilling, hydroxyl-amine), so-called *K* level has been identified (for refs see Strasser et al. 2004) in the time range between 0.01 and 0.5 ms.

For a large variety of leaves, and isolated chloroplasts, the relative fluorescence *F*/Fo at O-, J-, I-, and P (M) is found at 1 and around 3, 5, and 6, respectively (Strasser et al. 1995; Vredenberg et al. 2005). An alternative and commonly used parameter for characterizing the photosynthetic competence of a leaf or chloroplast preparation is the variable fluorescence Fv(= F − Fo) relative to the maximal fluorescence Fm(= Fm^{MTF}) at M (or P):Fv/Fm. According to this definition Fm/Fo ∼ 6 corresponds with Fv/Fm ∼ 0.83. In general, Fv/Fm-values around 0.8 (Fm/Fo ∼ 5) are considered to be representative of high performance and competence of the PSII machinery in leaves, green cells, and isolated chloroplasts. The availability of detection methods with improved sensitivity and time resolution has greatly contributed to identification of fluorescence characteristics and parameters (Schreiber 1983, 1986; Bolhar-Nordenkampf et al. 1989; Renger et al. 1995; Schreiber et al. 1995; Strasser et al. 1995; Reifarth et al. 1997; Kolber et al. 1998; Nedbal et al. 1999, 2000). Estimation of initial fluorescence yield and of rise kinetics with much higher precision and time resolution has become possible.

The kinetics of fluorescence changes at the onset of light pulses, varying in time range from ps to tens of seconds, has been the subject of many studies (for a survey see various chapters in Papageorgiou and Govindjee 2004). These studies among others have yielded information on rate constants and turnover of the primary quinone acceptor Q_A of PSII, and on heterogeneity and intersystem energy transfer (connectivity) among PSII units. Application of dedicated new photometric technologies (Schreiber 1986; Kolber et al. 1998; Nedbal et al. 2000) and of appropriate powerful routines in mathematical software have promoted the possibilities to resolve fluorescence responses in single (STF), twin (TTF), and multi turnover (MTF) excitations with higher time resolution and accuracy (Vredenberg et al. 2006, 2007).

Quantitative models relating variable PSII fluorescence and energy trapping have been the subject of many articles (Trissl et al. 1993; Dau 1994; Lavergne and Trissl 1995; Trissl and Lavergne 1995; Schreiber and Krieger 1996; Stirbet et al. 1998; Bernhard and Trissl 1999; Lazár 2006; Zhu et al. 2005). These models are based on the 'classic' concept that the energetic (open, closed) state of PSII

reaction centers is determined and quantified by the redox state of Q_A. In cases where the fluorescence yield is found to be at variance with the level predicted by Q_A^-, deviations have been interpreted in terms of

- heterogeneity (α-, β-, Q_B non-reducing-, inactive centers, etc.) within PSII (Melis and Homann 1976; Joliot and Joliot 1977; Anderson and Melis 1983; Black et al. 1986; Graan and Ort 1986; Chylla et al. 1987; Govindjee 1990; Lavergne and Leci 1993; Lavergne and Briantais 1996; Lazár et al. 2001; Tomek et al. 2003; Vredenberg et al. 2006);
- intersystem energy transfer (connectivity) (Joliot and Joliot 1964; Strasser 1978; Trissl and Lavergne 1995; Bernhardt and Trissl 1999);
- quenching of several types (non-photochemical, static, etc.) and/or by several components (e.g., P^+, Y_Z^+, Phe^-, Q_B^-, plastoquinone) (Butler 1972; Joliot and Joliot 1973; Vernotte et al. 1979; Klimov and Krasnovskii 1981; Krause et al. 1982; Hsu and Lee 1995; Kramer et al. 1995; Kurreck et al. 2000; Koblizek et al. 2001; Vasilév and Bruce 1998; Vredenberg 2004; Zhu et al. 2005)
- a double hit trapping mechanism based on the so-called Three State Trapping Model (TSTM) of PSII (Vredenberg 2000, 2004)).

The present article deals with a quantitative analysis of the initial phase of the MTF-induced fluorescence rise in the absence and presence of DCMU. Experimental curves are compared with the theoretical curve derived from the analytical solution of the differential equations dictated by the reaction pattern of primary electron transfer reactions at the acceptor and donor side of PSII as presented in Fig. 1. This analysis illustrates and quantifies why and how the kinetics of the initial fluorescence rise is determined by the rate constants of light excitation (k_L) and release of photochemical donor side quenching (k_{si}, $i = 0, \ldots, 3$). The analytical approach will be shown to give an adequate interpretation of the sigmoidal initial rise under conditions at which intersystem energy transfer is assumed not to occur.

Materials and methods

Experiments were performed on thylakoids isolated from leaves of *Chenopodium album* L. Conditions of plant growth and isolation of chloroplasts were described earlier (Hiraki et al. 2003). For isolation of thylakoids, leaves were harvested after about 1 month of growth in a growth chamber at a temperature of 22°C, a light period of 16 h per day, an irradiance level of 250 µmol photons m^{-2} s^{-1}, and a relative humidity of about 60%. Leaves were homogenized using a Sorvall Omnimixer in an isolation medium, containing 0.4 M sorbitol, 20 mM tricine-NaOH (pH 7.8), 10 mM NaCl, 5 mM $MgCl_2$, 2 mM sodium ascorbate and 2 mg/ml bovine serum albumin. After squeezing through three layers of nylon cloth, the chloroplasts were collected by centrifugation for 30 s at 3,000*g*, washed once in 50 mM sodium phosphate buffer (pH 7.8) to obtain broken chloroplasts, and finally collected by centrifugation during 5 min at 1,000*g*. The chlorophyll concentration in the stock suspension was adjusted to 2 mg Chl ml^{-1}.

Induction curves of chlorophyll fluorescence were measured with a Plant Efficiency Analyzer (either PEA-, or Handy PEA fluorometer, Hansatech Instruments Ltd, King's Lynn, Norfolk, UK) and viewed with dedicated software. Measurements were performed at room temperature. Fluorescence was excited with 1-s pulses of red light (650 nm) emitted with light-emitting diodes at maximal irradiance of about 650 W m^{-2} (approximately 3,300 µmol photons m^{-2} s^{-1}). Thylakoids were suspended in 0.5 ml reaction medium of 0.3 M sorbitol, 50 mM tricine-NaOH (pH 7.6), and 5 mM $MgCl_2$ at a Chl concentration of 10 or 20 µg ml^{-1} and kept in the dark. DCMU was added in complete darkness usually at a final concentration of 30 µM. It is assumed that the dark-adapted preparations have a $S_0/S_1 = 0.25/0.75$ heterogeneity (Hiraki et al. 2003). Fluorescence data were recorded at a sampling rate of 10 µs in the lower time range between 0.05 and 2 ms, and at lower rates in higher time domains. The experimental traces in general represent the averages of three samples each illuminated a single run. The following notations are being used in this article (see also abbreviations): $F(t)$: Fluorescence emission at time t; Fv(t)(= $F(t)$ − Fo): variable fluorescence at time t; rFv(= (F − Fo)/(Fm − Fo): relative variable fluorescence with $0 \leq$ rFv ≤ 1, in Strasser's models and interpretations rFv as defined here is termed V; nFv(= F − Fo)/Fo) normalized variable fluorescence.

Theory

The chain of reactions up to Q_A^- in a homogeneous system of separate dark-adapted PSII units (PSU II) with 100% open reaction centers (RCs) following a single picosecond (ps)-excitation is given in the upper row of Fig. 1. The state of the RC in a PSII unit is identifiable and characterized by the redox state of the acceptor and donor pair [Phe Q_A] and [Y_ZP], respectively, and by the number (i) of charges accumulated in the oxygen evolving complex (OEC), designated with $S_i(i = 0, \ldots, 3)$. When dark-adapted for 10–30 min, the PSUs in a system have been found to be heterogeneous with respect to their S-state with, as an average, S_1/S_0 is 0.75/0.25 (Vermaas et al. 1984).

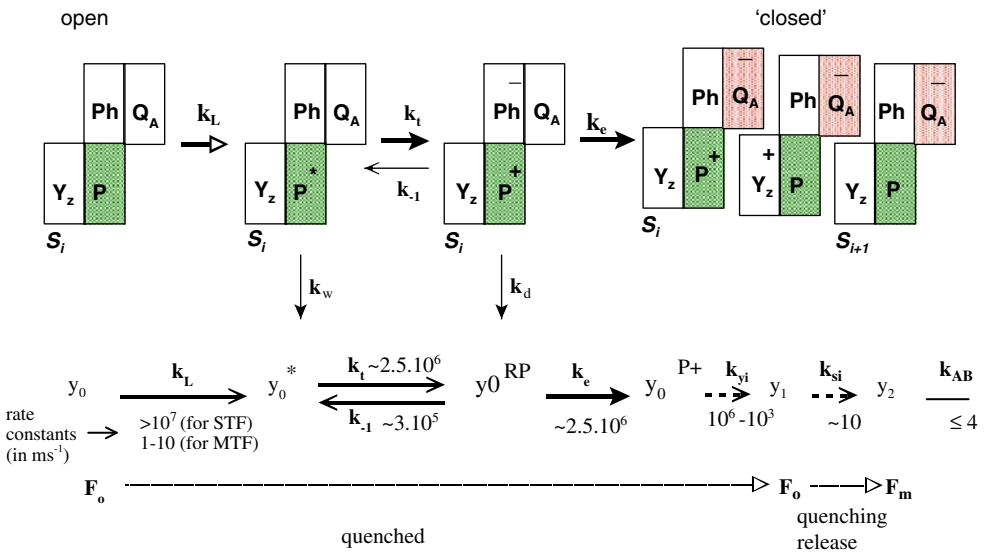

Fig. 1 *Upper section.* Representation of the reaction pattern and -intermediates associated with light driven transfer of dark-adapted open reaction center (RC) with oxygen evolving complex (OEC) in state S_i (designated with state S_i [Y_ZP Phe Q_A]) into its first quasi-stationary 'closed' state S_{i+1} [Y_ZP Phe Q_A^-] in green cells and chloroplasts. The term 'closed' refers to the indicated state with Q_A^- which in terms of the 'classic' 2-state trapping model is considered to be closed with rFv = 1(Fm^{STF}/Fo ~ 5); in terms of TSTM state S_{i+1} [Y_ZP Phe Q_A^-] has been called a semi-closed state with rFv = 0.5(Fm^{STF}/Fo ~ 3). Arrows (from left to right) mark the sequence light excitation, charge separation, Q_A reduction, Y_{Z^-} and OEC-oxidation with rate constants k_L, k_t, k_e, k_{yi}, and k_{si}, respectively, in which i(=1, …, 4) refers to the state S_i of the OEC. Oxidation of Q_A^- by Q_B is indicated with rate constant k_{AB}. The left-directed horizontal arrow marks charge recombination of radical pair P^+_{680}-Phe$^-$ with rate constant k_{-1}. Downward pointing arrows mark energy loss of P_{680}* and of P^+_{680}Phe$^-$ in a form different from photochemical storage with rate constants k_w and k_d, respectively. P_{680} is considered here as the traditional primary electron donor of PSII, ignoring that the accessory chlorophyll of the D1 protein has recently been identified to act as such (Groot et al. 2005; Holzwarth et al. 2006). This ignorance and simplification does not alter the outcome of the reasoning under the prevailing conditions that are discussed. *Middle section.* Reaction sequence (except for omission of non-energetic losses which are assumed to be comparatively small) for single-hit driven transfer of a system of dark-adapted PSUs, designated with y_0, with 100% open RCs and OEC in S_i state. Other designations refer to RC state drawn vertically above each. Typical values (in ms^{-1}) of the reaction rate constants are indicated (for survey see Zhu et al. 2005; Vredenberg 2004). The excitation rate for a single turnover flash (STF) and that commonly applied in a multi turnover light pulse (MTF) are also indicated. *Bottom section.* The release of donor side quenching associated with a change in fluorescence yield from Fo in PSU states y_0 through y_1 to Fm in state y_2 is indicated. The bottom line can also be read (see further text) as the reaction scheme $y_0 \rightarrow y_1 \rightarrow y_2$ in MTF excitation with rate constants k_L and k_{si} for the first and second step, respectively

The reaction scheme for the transfers of the RC upon a single turnover (STF) excitation is given in the second row of Fig. 1. The scheme is simplified by omitting the comparatively small dissipative and non-photochemical losses in antenna (k_w) and RC (k_d). Excitation (with rate constant k_L) causes the transfer of the dark-adapted 'open' state (y_0) via the excited (y_0^*) and 'radical pair' state (y_0^{RP}) to the electron-trapped (-stabilized) states y_0^{P+}, y_1, and y_2. With ps-laser STFs the excitation rate $k_L(\sim 10^9\ ms^{-1})$ exceeds the rate constant of photochemical trapping (charge separation) $k_t(\sim 10^7\ ms^{-1})$. In that case, the excited state y_0* can be considered to be identical with y_0. The transfer from y_0^{RP} to the state y_2 occurs via the intermediate states y_0^{P+} and y_1. The electron trapping efficiency Φ_{tr}^o in an excited open RC (y_o^{RP}) is $\Phi_{tr}^o = k_e/(k_e + k_{-1} + k_d) \sim k_e/(k_e + k_{-1})$ in which k_e, k_{-1}, and $k_d(<<k_e + k_{-1})$ rate are constants for Q_A photoreduction, radical pair recombination and non-radiative radical pair transfer, respectively (Fig. 1, second row). With typical values of the rate constants, (for a survey see Zhu et al. 2005), $\Phi_{tr}^o \sim 87\%$. One should keep in mind that an attenuation of the primary rate constant of Q_A reduction (k_e) or a stimulation of those of radical pair recombination (k_{-1}) or non-radiative recombination (k_d) results in a decrease in the usually high electron trapping efficiency of open centers (Φ_{tr}^o). Conversely, a temporary decrease in k_{-1} with unaltered k_e will cause a transient increase in Φ_{tr}^o.

The time pattern of generation and decay of each of the intermediate RC states in the photochemical reaction chain follows from the solution of a system of ordinary linear differential equations (ODE) associated with the reaction scheme. These have been presented in detail elsewhere (Vredenberg 2004). Analytical solution of these equations yields expressions for y_0, y_0^*, y_0^{RP}, y_0^{P+}, y_1, and y_2 as a function of time (see also Trissl 2002 for an elementary mathematical exposure). The transient state y_1 and the final

photochemical product (y_2), under conditions at which Q_A^- oxidation is blocked, are formed within tens of ns and μs, respectively (data not shown, but see Vredenberg 2004).

The concept of PSU closure by a single photon hit requires additional assumptions to conform the kinetics of the variable fluorescence to the theoretical predictions. The single turnover induced transfer of an open reaction center into states with Q_A^- (Fig. 1) is accompanied by an approx. threefold increase in fluorescence yield from the minimal dark level Fo to $Fm = Fm^{STF} \sim 3Fo$ (Vredenberg et al. 2006, 2007, and references therein). This increase has been ascribed to the release of photochemical quenching by Q_A due to its reduction to Q_A^- (Duysens and Sweers 1963).

The kinetics of the ns-STF-induced variable fluorescence in intact cells and chloroplasts have shown a biphasic rise in the 0.1–100 μs and a multiphasic recovery in the 0.05–10^4 ms time range, respectively (Mauzerall 1972; Steffen et al. 2005; Belyaeva et al. 2006). The kinetic pattern of the recovery phase is similar to that of STF- and TTF-induced responses (Nedbal et al. 1999; Vredenberg et al. 2006; 2007) with a major fast phase in the 0.05–1 ms time range ascribed to quenching recovery in association with Q_A^- reoxidation in Q_B reducing RCs. A major part of the rise has been found to occur within tens of μs. The substantial attenuation of the STF-induced rise with respect to excitation in the ns time range has been ascribed to fluorescence quenching by reaction intermediates at the donor side like P^+ (Butler 1972), Y_Z^+ (Vredenberg et al. 2002) and others (Steffen 2003). Following terminology introduced by others (Schreiber and Neubauer 1987), fluorescence quenching by electron transport intermediates at the donor side is called donor side quenching (DSQ). The fact that the retarded fluorescence rise in STF excitation occurs in the same time range as reported for the $y_1 \rightarrow y_2$ state transfer (see Fig. 1, second row) has been interpreted as evidence that this rise DSQ, is the reflection of the release of donor side quenching (Hiraki et al. 2004; Vredenberg 2004). The interpretation of dealing with DSQ that is caused by Y_Z^+ is supported by the observations that the amplitude of STF- and TTF-induced variable fluorescence responses is characterized by a period-of-four oscillation pattern associated with the four-step oxidation of water via the *S*-states of the OEC that are oxidized by Y_Z^+ (Schreiber and Neubauer 1988; Kolber et al. 1998; Shinkarev 2004; Vredenberg et al. 2006, 2007). However, it is important to keep in mind that it is the rate constant of the release rather than the identity of the quencher associated with DSQ which determines the kinetics in the 0–0.2 ms time range of the OJDIP induction curve.

Continuous illumination with a 1 s multi turnover light pulse (MTF excitation) of a dark-adapted homogeneous system of PSUs with open RCs and equal antenna size will cause an inductive transfer of the system into one with reduced (Q_A^-) centers. The events caused by the first excitation of the MTF can be described a priori by the same set of rate equations as given for RC transfer in an individual PSU (Fig. 1), if intersystem exciton transfer, quantified by the connectivity-related parameter p (Joliot and Joliot 1964; Strasser 1978; Trissl and Lavergne 1995), is assumed to be zero, i.e., $p = 0$. The identification of the RC states $y_j (j = 0, \ldots, 2)$ in the first of a multi-turnover excitation then refers to the fraction of PSUs in which the RCs are in the y_j-state (see Fig. 1). The fluorescence during this transfer will rise from the initial low level Fo to a maximal level $Fm(=Fm^{STF})$, corresponding to the yields of a system with 100% open (y_0) and 'closed' (y_2) PSUs, respectively. With equal antenna size, independent (separate) PSUs, a single hit trapping mechanism and disregarding quenchers other than Q_A, one would expect a $F(t)$ curve proportional to the growth curve of PSUs with Q_A^--containing centers (see Strasser et al. 2004; Vredenberg 2004). The subsequent events in the time domain beyond 2 ms during a multi-turnover (MTF) excitation cause a further transfer of the y_2 state associated with an increase in Fm towards a maximum with $Fm^{MTF} \sim 5$ Fo (Vredenberg 2004; Vredenberg et al. 2006).

The average duration time of an excitation of the photosystems during a multi-turnover light pulse, is determined by antenna size, intensity of the pulse, density of the sample, i.e., Chl concentration [Chl], and the optical path length. The inverse of this time is termed the excitation rate (frequency), k_L. Under usual experimental conditions, the excitation rate in the commonly used commercial instruments (Hansatech, Walz) is in the range between 1 and 10 ms^{-1}. Recently a high intensity modification of a Hansatech fluorometer has become available in which $k_L \sim 20\ ms^{-1}$ at maximal power (Schansker et al. 2006). With the excitation rate in this range, k_L is of the same order of magnitude as the rate constant k_{s_1} of the release of donor side fluorescence quenching (DSQ), probably coinciding with that of Y_Z^+ reduction (OEC oxidation), in state S_i. It is several orders of magnitude lower than the rate constants of the primary electron transfer reactions (for a survey, see Dau 1994; Vredenberg 2004; Zhu et al. 2005). The first reliable data point of the fluorescence signal (when measured with a PEA) is at 50 μs and, with $k_L = 5\ ms^{-1}$, each turnover excitation will take about 200 μs. This means for these conditions with $k_L << k_e < k_t$ and with $\Phi_{tr}^o (= k_e/(k_e + k_{-1}) \sim 1$, and assuming that the major fraction of RCs is in S_1 state, that the reaction pattern $y_0 \rightarrow y_0^* \rightarrow y_0^{RP} \rightarrow y_0^{P+} \rightarrow y_1 \rightarrow y_2$ (see Fig. 1) can be represented by a scheme $y_0 \rightarrow y_1 \rightarrow y_2$ with rate constants k_L and k_{s_1} for the first and second step, respectively. The three ODEs for each of the reaction partners in the scheme are $\frac{dy_0}{dt} = -k_L y_0, \frac{dy_1}{dt} = k_L y_0 - k_{s_1} y_1$, and $\frac{dy_2}{dt} = k_{s_1} y_1$. These give the following analytical

solution (for an extensive derivation the reader is referred to Trissl (2002) and to Vredenberg (2004)):

$$y_0(t) = \mathrm{e}^{-k_L t} \tag{1}$$

$$y_1(t) = \frac{k_L}{k_{s1} - k_L}(\mathrm{e}^{-k_L t} - \mathrm{e}^{-k_{s_1} t}) \tag{2}$$

$$y_2(t) = 1 - \frac{k_{s_1}}{k_{s_1} - k_L}\mathrm{e}^{-k_L t} + \frac{k_L}{k_{s_1} - k_L}\mathrm{e}^{-k_{s_1} t} \tag{3}$$

The same scheme and set of equations hold if the electron trapping efficiency $\Phi_{tr}^{o} < 1$. In that case, the $y_0 \rightarrow y_1$ transition occurs with an attenuated rate constant $k_L^* = \Phi_{tr}^{o} k_L$.

If it is assumed, following evidence derived from ns laser-induced $F(t)$ kinetics discussed earlier, that the fluorescence yield in y_1(= [Y_Z^+P Phe Q_A^-]) does not differ much (Steffen et al. 2005), if at all, from that of y_0 due to effective DSQ, one expects that the relative fluorescence induction curve rFv(t)(= [$F(t)$ − Fo]/(Fm − Fo)) will coincide with $y_2(t)$, i.e., rFv(t) = $y_2(t)$. It is obvious from Eq. 3, and illustrated in Fig. 2a, that the initial fluorescence rise kinetics at a given value of k_{s_1} are dependent on k_L and vice versa. The rise shows a substantial delay when $k_L \sim k_{s_1}$ and approaches an exponential rise at the extremes $k_L \ll k_{s_1}$ (Fig. 2a) and $k_L \gg k_{s_1}$ (not shown). It follows from Eq. 3 (see Appendix A):

$$y_2(t) = 1 - \mathrm{e}^{-k_L t}(1 + k_L t) \tag{3a}$$

for $k_L = k_{s_1}$,

$$y_2(t) \approx 1 - \mathrm{e}^{-k_L t} \tag{3b}$$

for $k_L \ll k_{s_1}$, and

$$y_2(t) \approx 1 - \mathrm{e}^{-k_{s1} t} \tag{3c}$$

for $k_L \gg k_{s_1}$. Equation 3c signifies that the $F(t)$ rise is independent of intensity at high excitation rate k_L and illustrates, in agreement with the $F(t)$ response in a ns laser flash (Steffen 2003), its sole dependence on the rate constant (k_{s_1}) of donor side quenching (DSQ) release under these conditions. The laser-induced excitation data (Steffen

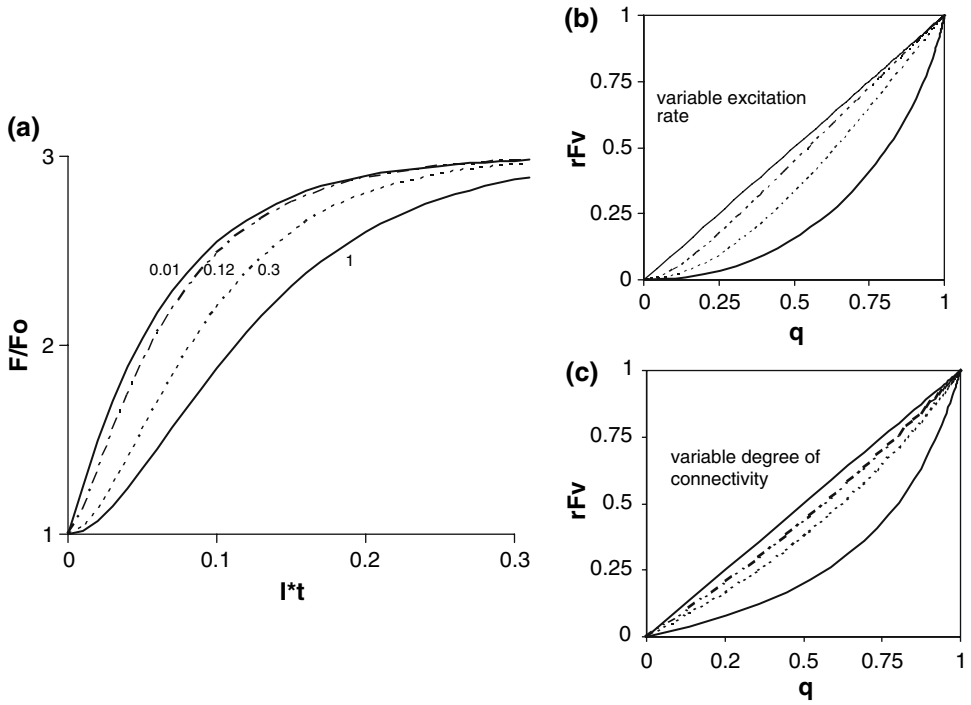

Fig. 2 (**a**) Accumulation of state $y_2(t) = 1 - \frac{k_{s_1}}{k_{s_1} - k_L}\mathrm{e}^{-k_L t} + \frac{k_L}{k_{s_1} - k_L}\mathrm{e}^{-k_{s_1} t}$(Eq. 3), representing the release of fluorescence quenching (expressed as $F(t)$/Fo) = 1 + nFv^{STF} × $y_2(t)$ (Eq. 8 with nFv^{STF} ∼ 2) plotted as a function of incident energy $I \times t$ (I is incident light intensity) at variable excitation rates (intensities) k_L, relative to an assumed rate constant of donor side quenching release $k_{s_1} = 15\ \mathrm{ms}^{-1}$. k_L(= $\alpha \times k_{s_1}$) was attenuated with factor α = 1, 0.3, 0.12, and 0.01 (curves from bottom to top). With $\alpha = 1 (I = 100\%)$ the numbers on the $I \times t$-axis can be read in ms units. (**b**) The relative variable fluorescence yield rFv(= $y_2(t)$) plotted as a function of the fraction B(=q) of RCs with Q_A^- ('closed') with $q = 1 - e^{-k_L t}$ (Eq. 5). Calculated curves (from bottom to top) are for α = 1, 0.3, 0.1, and 0.01. (**c**) Change in fluorescence yield calculated for different degrees of assumed connectivity between RCs with rFv = $\frac{q}{1 + C_{hyp}(1-q)}$ as a function of the fraction q of RCs with Q_A^- ('closed'). Calculated curves (from bottom to top) are for C_{hyp} = 3.5, 0.65, 0.2, and 0. Figure shows effect of excitation rate k_L on (a) the sigmoidicity of the initial rise, (b) non-linear relationship between variable fluorescence and fraction q of RCs with Q_A^- ('closed'), except at low excitation rates ($\alpha << 0.1$) and (c) the 'classic' hyperbolic relation between variable fluorescence and fraction of closed centers is, for a fixed excitation rate (intensity) and C_{hyp}-value, different from the one dictated by the reaction scheme which incorporates donor side quenching release (Eq. 3)

2003; Belyaeva et al. 2006) suggest $k_{s_1} \sim 30\ \mathrm{ms}^{-1}$. Similarly Eq. 3b is representative for the exponential rise in variable fluorescence measured at low intensity (excitation rate) (Lavergne and Leci 1993; Tomek et al. 2003).

The fraction q^{dsq} of RCs in which the acceptor and donor side quenching is released is equal to

$$q^{\mathrm{dsq}}(t) = \frac{y_2}{y_0 + y_1 + y_2} = y_2(t) \tag{4}$$

(see Eq. 3)

It is different from the fraction q of ('closed') RCs in which acceptor side quenching is released, i.e., with Q_{A}^{-}

$$q(t) = \frac{y_1 + y_2}{y_0 + y_1 + y_2} = 1 - y_0(t) = 1 - \mathrm{e}^{-k_{\mathrm{L}}t} \tag{5}$$

(see Eq. 1)

Thus the relative variable fluorescence rFv(= y_2), in contrast to being linear with the fraction q^{dsq} of RCs in which quenching is released (Eq. 4), is non-linearly related with the fraction q of closed (Q_{A}^{-} containing) RCs (Eq. 5), except for the extremes of excitation rate (Eqs. 3b and 3c). This result is on first sight remarkable for a system that has been assumed to operate without intersystem exciton transfer ($p = 0$). A non-linear relation between rFv and the fraction q of closed (Q_{A}^{-} containing) RCs which commonly is found for experimental $F(t)$ curves measured in the presence of DCMU is routinely interpreted as an indicator and illustration of intersystem energy transfer (connectivity) between PSII units (e.g., Strasser 1978; Lavergne and Trissl 1995). A closer analysis of these two fundamentally different rFv versus q relationships and the likelihood that the contribution of connectivity between PSUs to the apparent non-linearity between normalized variable fluorescence and the fraction of closed RCs is small, if not negligible is presented in the Appendix B.

Figure 2b shows the graphs of rFv(=$y_2(t)$) plotted as a function of q for different values of k_{L}, attenuated relative to k_{s_1} (=15 ms^{-1}) with variable factor $\alpha(k_{\mathrm{L}} = \alpha k_{s_1})$. Combination of Eqs. 1, 3, and 5 gives the expression of the relative variable fluorescence rFv(=y_2) as a function of the fraction q of centers with Q_{A}^{-}.

$$\mathrm{rFv} = \frac{q - \alpha \times [1 - (1-q)^{1/\alpha}]}{1 - \alpha} \tag{6}$$

with $\alpha = k_{\mathrm{L}}/k_{s_1}$. For $k_{\mathrm{L}} = k_{s_1}$ ($\alpha = 1$, see Appendix A)

$$\mathrm{rFv} = q + (1-q) \times \ln(1-q) \tag{6a}$$

It follows easily from Eq. 6 that rFv = q for $\alpha \ll 1$; the condition rFv = q is found to be reached (not shown) for $\alpha < 0.05$. For each value of α with $1/\alpha = 1, 2, 3$, etc., the rFv versus q relation (Eq. 6) is a higher order polynomial. For instance for $1/\alpha = 2$ and 4, $\mathrm{rFv} = q^2$ and $2q^2 - 1.3q^3 + 0.3q^4$, respectively. Illustrated curves in Fig. 2b are (from bottom to top) for $\alpha = 1$, 0.3, 0.12 and 0.01. Figure 2c shows, for comparison, the graph of the amply documented intensity-(k_{L}-) independent hyperbolic relation between change in fluorescence yield rFv and the fraction q of RCs with Q_{A}^{-} ('closed') calculated for different degrees of connectivity between RCs, expressed by the parameter $C_{\mathrm{hyp}} = \mathrm{nFv} \times p$ (Strasser 1978, 2004), with

$$\mathrm{rFv}(q) = \frac{q}{1 + C_{\mathrm{hyp}}(1-q)} \tag{7}$$

Calculated curves (from bottom to top) are for $C_{\mathrm{hyp}} = 3.5$, 0.65, 0.2 and 0. The major difference between the plots of Fig. 2b and c is that the rFv versus q in the latter is independent of light intensity. Besides, it is clear that even at a fixed light intensity (k_{L}), a theoretical $F(t)$ curve (Fig. 2a), incorporating the effect of donor side quenching, cannot be matched with a corresponding hyperbolic function associated with a certain value of $C_{\mathrm{hyp}}(p)$. The hyperbolic relation (Fig. 2c) gives too high values of the variable fluorescence at q-values below 0.5.

Thus, depending on trapping efficiency, rates of excitation (k_{L}) and quenching release (k_{si}) and independently of energy transfer among PSUs, the fluorescence induction curve $F(t)$ shows a delay in the rise, due to donor side quenching which is released with a rate constant of the order of tens of ms^{-1} (Steffen 2003). Interestingly and documented in detail in Appendix C, the theoretical rFv versus q relation is nonlinear in MTF excitation (in the presence of DCMU) under conditions at which the effect of donor side quenching and intersystem connectivity is negligible and a double hit trapping mechanism is adopted. Fig. 3 shows the result of the rFv versus q relation under these conditions according to Eqs. C.3 and C.4 (see Appendix C). This curve gives the closest match with the one for the hyperbolic relation (see Eq. B.1) when one takes $C_{\mathrm{hyp}} \sim 0.3$ which corresponds with $p \sim 0.08$.

Results and interpretation

Figure 4 shows the 1 s MTF-induced $F(t)$ curves of a dark-adapted chloroplast preparation in the 0.05 ms to 1 s time range in the absence and presence of 30 μM DCMU. The figure illustrates, in agreement with many reports (Schreiber and Neubauer 1987; Lazar and Pospisil 1999; Hiraki et al. 2003), that addition of DCMU in the dark causes, as compared to the dark control, (i) an increase in the initial fluorescence level, measured here at $t = 50$ μs and close to $F(0)$ (see below), (ii) a lower maximal level $\mathrm{Fm}^{\mathrm{MTF}}$, and (iii) an enhancement of the initial fluorescence rise which is shown in more detail in Fig 5. The increase in Fo and decrease in $\mathrm{Fm}^{\mathrm{MTF}}$ upon DCMU additions has been reported to be absent in preparations that have been

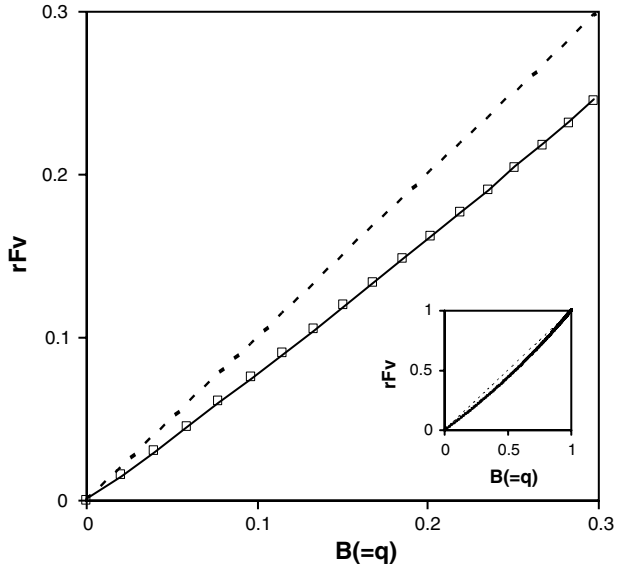

Fig. 3 The relative variable fluorescence yield rFv(t) (Eq. C.3 in Appendix C) plotted against the corresponding normalized area $B(t)$ (Eq. C.4) above rFv(t) (solid line) in the $B(t)$-range from 0 to 0.3, simulated for MTF excitation at excitation rate k_L far below the rate constant k_{s_1} of donor side quenching release and adopting a double hit trapping mechanism. The symbols are for the same virtual situation adopting a single hit trapping mechanism in which $\mathrm{rFv} = \frac{q}{1+C_{\mathrm{hyp}}(1-q)}$ (Eq. B.1 in Appendix B) with $C_{\mathrm{hyp}} = 0.30$ for a best fit with the solid line. The insert shows the plots in the full range. In this case the best fit between both curves is for $C_{\mathrm{hyp}} = 0.28$. Dashed curves are for the linear relation $\mathrm{rFv} = B$ with $C_{\mathrm{hyp}} = 0$. B is the fraction q of RCs with Q_A^-

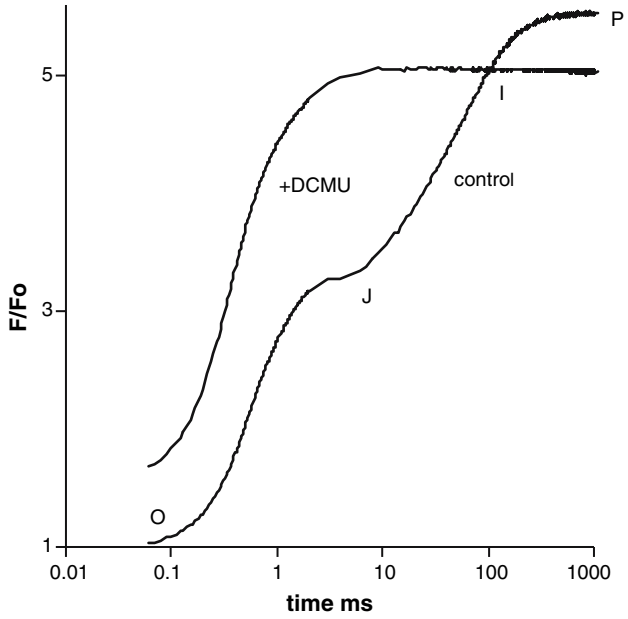

Fig. 4 Direct recordings (average of 3 and plotted on a log time scale) of the fluorescence induction in approximate F/Fo units of 10–15 min dark-adapted *Chenopodium* chloroplasts (10 µg chl/ml) in a 1 s light pulse in the 0.05 ms to 1 s time range, in the absence (control, OJIP) and presence of 30 µM DCMU (+DCMU), respectively. Figure shows (i) the amply documented increase in $F(0)$ (in this case recorded at 0.05 ms) after addition of DCMU relative to Fo in the absence of the inhibitor with $F(0)/\mathrm{Fo} \sim 1.6$, and (ii) decrease in $\mathrm{Fm}^{\mathrm{MTF}}$

adapted in the dark for more than 12 h (Toth et al. 2005; Haldimann and Tsimilli 2005). The initial fluorescence rise kinetics in the 0–0.2 ms time range of leaves and chloroplast preparations, under conditions in which exciton transfer among PSUs is assumed to be absent, are theoretically dictated by the fraction q^{dsq} of RCs in which donor- and acceptor quenching has been released (Eqs. 3 and 4), and by the amplitude $\mathrm{Fv}^{\mathrm{STF}}$ of the variable fluorescence upon STF excitation in which Q_A has become reduced. After normalization one obtains $\mathrm{nFv}^{\mathrm{STF}} = \mathrm{Fv}^{\mathrm{STF}}/\mathrm{Fo} = \mathrm{F}^{\mathrm{STF}}/\mathrm{Fo} - 1(\sim 2)$. Thus the initial phase of the experimental curve $F(t)$ in the absence of DCMU should match in first approximation a theoretical relation which follows from Eq. 3 with

$$\begin{aligned}\frac{F(t)}{\mathrm{Fo}} &= 1 + \mathrm{nFv}^{\mathrm{STF}} \times q^{\mathrm{dsq}}(t) \\ &= 1 + \mathrm{nFv}^{\mathrm{STF}} \\ &\quad \times \left(1 - \frac{k_{s_1}}{k_{s_1} - k_L} e^{-k_L \times t} + \frac{k_L}{k_{s_1} - k_L} e^{-k_{s_1} \times t}\right) \end{aligned} \quad (8)$$

For reasons of simplicity, the rate constant k_{s_0} of donor side quenching release in the S_0 fraction (β) in this approximation has been taken equal to that (k_{s_1}) of the S_1 fraction ($1 - \beta$). It has been evidenced (Vredenberg et al. 2006) that the β- (So) fraction in dark-adapted preparations is populated with Q_B-nonreducing RCs. These have been shown to become double reduced upon twin (TTF) excitation (Vredenberg et al. 2007). It has been assumed, and justification for this can be read from the bottom curve in Fig. 5, that in control chloroplasts the contribution of double reduction in the β-fraction to the fluorescence kinetics in the 0–0.2 ms time range is negligible. In the presence of DCMU, both fractions β and $(1 - \beta)$, have become Q_B-nonreducing and susceptible to double reduction in a second excitation (Vredenberg et al. 2006, 2007). The double reduction will contribute to the kinetics of the initial $F(t)$ rise in the presence of DCMU. Reduction of the single reduced fraction is assumed to occur at an attenuated excitation rate with rate constant $k = \phi_{\mathrm{tr}}^{\mathrm{sc}} \times k_L$, due to the relatively low electron trapping efficiency $\phi_{\mathrm{tr}}^{\mathrm{sc}}$ in reduced (semi-closed) RCs (Vredenberg 2004). The reduction results in the closure of the RCs. It is accompanied by a quenching release that can be approximated (Eq. 3b) to occur with rate constant $k(=\phi_{\mathrm{tr}}^{\mathrm{sc}} \times k_L)$ because excitation rate $k(=\phi_{\mathrm{tr}}^{\mathrm{sc}} \times k_L)$ is small as compared to k_{s_1} and k_{s_2}. The variable fluorescence $F^{[2]}(t)$ associated with quenching release in the second excitation is given by

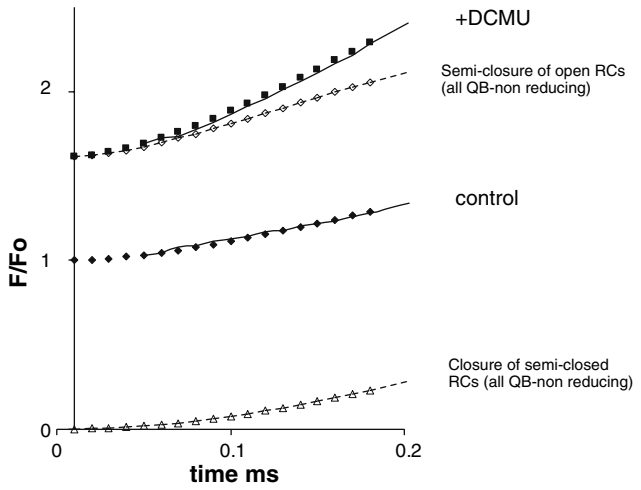

Fig. 5 Same recording as in Fig. 4 of the initial phase of the fluorescence induction of *Chenopodium* chloroplasts in a 1 s light pulse in the 0(50) to 250 μs linear time range in the absence (middle solid curve) and presence (upper solid curve) of DCMU, respectively. Closed symbols are graphs of the functions which give the closest match with the experimental curve in the 50–200 μs time range. For the control curve (closed diamonds) the function is of Eq. 8 with nFv = 2.2, $k_L = 1.8$ and an assumed rate constant of donor side quenching release 20 ms^{-1}. For the DCMU curve (closed squares) the function is of Eq. 10 with the same values for nFv and k_{s_1} and with $k_L = 3.2$ ms^{-1}, $\beta = 0.34$ and $\phi = 0.52$. The matching curve is the sum of that of Eq. 8 (open diamonds) and of Eq. 9 (*open triangles*). These represent the single and double reduction of the Q_B-nonreducing RCs in the presence of DCMU

$$F^{[2]}(t) = q^{\mathrm{dsq}}(t) \times \mathrm{Fv}^{\mathrm{STF}} \times \left(1 - \mathrm{e}^{-\Phi_{\mathrm{tr}}^{\mathrm{sc}} k_L t}\right) \tag{9}$$

After summation of Eqs. 8 and 9 and incorporating the offset of Fo, the initial rise of the fluorescence increase (quenching release) in the presence of DCMU can be approximated by the expression

$$\frac{F^{[\mathrm{dcmu}]}(t)}{\mathrm{Fo}} = 1 + \beta \times \mathrm{nFv}^{\mathrm{STF}} + \mathrm{nFv}^{\mathrm{STF}} \times q^{\mathrm{dsq}}(t) \times \left(2 - \mathrm{e}^{-\Phi_{\mathrm{tr}}^{\mathrm{sc}} k_L t}\right) \tag{10}$$

β equals the relative size of the (reduced) S_0 fraction with Q_A^- in the DCMU treated dark-adapted state. The factor $\beta \times \mathrm{nFv}^{\mathrm{STF}}$ is the size of the change in the initial fluorescence level in the dark at the onset of MTF illumination. This experiment shows $\beta \times \mathrm{nFv}^{\mathrm{STF}} \sim 0.6$ which corresponds, with $\mathrm{nFv}^{\mathrm{STF}} \sim 2$, with an approx. 30% S_0 fraction. This is in the range usually found for chloroplasts that have been dark-adapted for 5–60 min. In the absence of the herbicide, all reductive electrons in the Q_B-nonreducing S_0 fraction (β) are assumed to be on Q_B. Double reduction in these RCs occurs at a low initial rate because of the low electron trapping efficiency $\Phi_{\mathrm{tr}}^{\mathrm{sc}}$ (Eq. 9) of single reduced RCs in S_0, as has been assumed before.

The analysis of fluorescence data in the absence and presence of DCMU, with application of Eqs. 8 and 10, is shown in Fig. 5. It shows that the experimental data of the fluorescence increase in the 50–150 μs time range in the absence of DCMU are in quantitative agreement (Eq. 8) with an initial event associated with release of photochemical quenching that occurs with an assumed rate constant $k_{s_1} = 20$, with light excitation at a rate $k_L = 1.8$ ms^{-1}, and with $\mathrm{nFv}^{\mathrm{STF}} \sim 2.2$. Extrapolation of the theoretical curve gives the initial level Fo = 1 at $t = 0$. Similarly one finds, at the same rate of quenching release ($k_{s_1} = 20$ ms^{-1}) a theoretical fit with excitation rate $k_L = 3.2$ ms^{-1} and, after extrapolation, an initial fluorescence level $F(0) = 1.6 \times$ Fo in the presence of DCMU. The higher rate of fluorescence increase (quenching release) in the presence of DCMU is in agreement with amply documented observations (Vredenberg 2000; Hiraki et al. 2003, 2004). This effect is presumed to be due to the release of a sub-optimal electron trapping efficiency $\Phi_{\mathrm{tr}}^{\mathrm{o}}(= k_e/(k_e + k_{-1}))$ in open centers by the inhibitor. With reported literature values for k_e, k_{-1}, and k_d (for survey see Zhu et al. 2005), $\Phi_{\mathrm{tr}}^{\mathrm{o}} \sim 0.87$. If, for as yet unknown reasons, the actual rate constant of primary Q_A reduction in the dark-adapted control chloroplast preparations is tenfold less than the reported optimal value $k_e = 3.10^6$ ms^{-1}, the electron trapping efficiency in the PSII RCs is reduced to $\Phi_{\mathrm{tr}}^{\mathrm{o}} \sim 0.5$. The electron trapping efficiency at the acceptor side controls the rate at which the release of donor side quenching occurs. The increase in the rate of quenching release after DCMU addition is not caused, in contrast to what in a comparable situation has been proposed (Joliot and Joliot 2002; Rappaport et al. 2007), by the inhibition of Q_A^- oxidation. The scheme of Fig. 1 predicts that the initial $F(t)$ rise is not affected by the rate of Q_A^- oxidation.

Figure 6 shows the data (symbols) of the fluorescence increase $F(t)$/Fo in the presence of DCMU plotted as a function of the incident actinic energy flux $I \times t$ in the range between 0 and 1 at two intensities (I) different by a factor 4 and indicated with 100% and 25%. The $I \times t$ range for $I = 100\%$ and 25% corresponds to the time range from 0 to 1 and 4 ms, respectively. The lines are the graphs of the theoretical curve (Eq. 3) calculated for the $y_0 \rightarrow y_2$ transition with $\mathrm{Fm}^{\mathrm{STF}}/\mathrm{Fo} = 3$ and rate constant pairs (k_L, (k_L, k_{s_1}) (3, 9) and (0.7, 9) for the 100% and 25% light intensities, respectively. The initial change in fluorescence emission (yield) at equal energy flux is, in agreement with the theoretical prediction (Eq. 3), dependent on the intensity of the incident light. The figure shows that the 'degree' of sigmoidicity of the $F(t)$ curve is dependent on the intensity of the actinic light and decreases with a decrease in excitation rate k_L (intensity). This agrees nicely with Eqs. 3 and 3a. Curves measured at 50% and 75% of full intensity were found to be intermediate between those of the two extremes shown here. The inset at the right hand side of Fig. 5 (reproduced from Ronald Steffen's PhD thesis, Berlin 2003) shows the $F(t)$ kinetics in a single

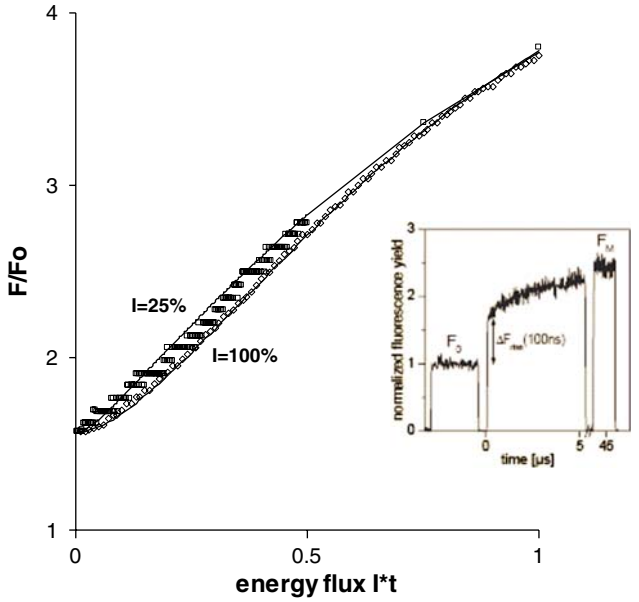

Fig. 6 Fluorescence increase (symbols) in dark-adapted *Chenopodium* chloroplasts (10 µg chl/ml) in the presence of DCMU at 100% (lower curve) and at 25% of incident intensity (I) plotted as function of light flux $I \times t$. $I \times t = 1$ for full intensity corresponds with $t = 1$ ms, which means for $I = 25\%$ with $t = 4$ ms. Solid lines are the fits of the experimental curves, calculated with TSTM and application of Eq. 10 (Hiraki et al. 2003; Vredenberg 2004). The figure shows that the sigmoidicity is less at a lower intensity (excitation rate k_L) The right hand insert shows a laser flash induced increase in fluorescence in spinach chloroplasts, relative to Fo, in the time range from 0–45 µs (reproduced from Fig. 28 in Steffen 2003). Note that in the laser flash the maximum fluorescence (Fm^{STF}) at 45 µs relative to Fo is $Fm^{STF}/Fo \sim 2.4$, whereas in a 1 s MTF $Fm^{MTF}/Fo \sim 5$ (see Fig. 4)

ns-laser flash ($k_L \sim 10^6$ ms^{-1}). It shows the absence of sigmoidicity for the major component, conclusive with the theoretical prediction expressed in Eq. 3c. Thus the usually observed sigmoidicity in fluorescence induction curves in high intensity light pulses in the presence and absence of DCMU, like that illustrated in Figs. 4 and 5, cannot be used as an exclusive indicator of intersystem connectivity synonymous with the operation of the 'lake model' of energy trapping as is commonly done.

Discussion

Photochemical electron trapping in PSII (Fig. 1) and the analytical solution of the underlying linear rate equations (Eqs. 1–3), implicating the assumed absence of connectivity between units, predict, in agreement with the experimental results (Figs. 5 and 6), a sigmoidal rise of the MTF-induced fluorescence response curve. The sigmoidicity arises from the fact that the variable fluorescence Fv is controlled by the rate constant of light excitation k_L and of release of donor side quenching k_{s_1}. Characteristics of donor side quenching can be read from the rise and decay kinetics of quenching release in ultra short single turnover excitations (Butler 1972; Mauzerall 1972; Steffen 2003; Steffen et al. 2005; Belyaeva et al. 2006). The 'degree' of sigmoidicity of $F(t)$ is determined by the ratio between k_L and k_{s_1} (Figs. 2, 6). It decreases with k_L/k_{s_1} ratio far above or below 1 (Eqs. 3b and 3c). The absence of sigmoidicity in the $F(t)$ curve in short STFs ($k_L > 10^6$ ms^{-1}) with, except for a minor ns component, an approx. exponential rise in the 10–50 µs time range (Steffen 2003) agrees qualitatively with the theoretical predictions expressed in Eqs. 3 and 3b. It is not surprising that in general MTF-induced $F(t)$ curves have been found to be sigmoidal. This presumably is because most of this type of fluorescence experiments reported so far have been done with either home-built or commercially available set-ups in which, under optimal conditions the light excitation rate during a light pulse will have been close to the rate constant of quenching release. For instance, with a chloroplast density of 10 µg chl/ml, a RCII density of 0.004 and at a photon fluency rate of 0.4 µmol/cm^2 s, $k_L \sim 10$ ms^{-1} which is close to that of the quenching release (k_{s_1}) which we find in the range between 10 and 20 ms^{-1}.

Energy transfer between PSII units, usually denoted as PSII connectivity or grouping (Joliot and Joliot 1964; Strasser 1978), has been recognized for its influence on the fluorescence induction curve in particular the initial phase in the presence of DCMU (Melis and Homann 1976; Geacintov and Breton 1987; Lavergne and Trissl 1995). In the 'classical' concept the relation between the fraction q of centers with Q_A^- and the variable fluorescence yield is non-linear (i.e., hyperbolic) if there is energy transfer (connectivity) between units. The connectivity theory predicts that the degree of sigmoidicity is independent of light excitation rate (Eq. B.1 in Appendix B). Our data show (Fig. 6) a decrease in the degree of sigmoidicity with a decrease in light intensity (excitation rate). This is conclusive with the kinetic theory of electron supply and -trapping at donor- and acceptor side of PSII, respectively (Figs. 1 and 2), if donor side fluorescence quenching below P^+ is taken into account. It is necessary to discriminate between the clear 'sigmoidicity' effect due to donor side-quenching at excitation rates different from the rate constant of the release of this quenching by one order of magnitude, and that associated with intersystem connectivity. It has been reported for thylakoids in the presence of DCMU (Rappaport et al. 2007) that the relative variable fluorescence rFv and the normalized area above rFv, which equals the fraction of 'closed' RCs (i.e., with Q_A^-), when plotted on a $I \times t$ scale, vary with the incident intensity (I). This means (data not shown) that the plot of rFv versus fractions of closed RCs from which the connectivity-related parameter C_{hyp} (Eq. 7,

Fig. 2) is calculated varies with intensity which would mean that connectivity is dependent of light intensity. This is in conflict with the theory which rules out such intensity dependency. In addition, it should be considered that the routinely used method of estimating the parameter from the relation between the rFv(t) and the normalized area $B(t)$ above rFv(t) in DCMU-treated samples (Strasser 1978) needs a correction for the nonlinearity which arises when a double hit trapping mechanism like TSTM is adopted (Vredenberg 2000, 2004). In that case, as outlined in Appendix C and illustrated in Fig. 4, a nonlinearity is apparent which is identical to that with a connectivity-related parameter $C_{\mathrm{hyp}} \sim 0.30$ if a single hit trapping mechanism is adopted and donor side quenching is negligible.

There is as yet no clear experimental proof to confirm the hypothesis that DSQ is governed by Y_Z^+. This would require simultaneous measurements of STF-induced Y_Z^+ reduction and of time resolved ns-STF-induced variable fluorescence at a higher precision and accuracy than hitherto reached. The availability of such experiment would allow a comparison of the $F(t)$ response with the theoretical curve $\frac{F(t)}{\mathrm{Fo}} = \mathrm{nFv}^{\mathrm{STF}} \times (1 - \mathrm{e}^{-k1\times t}) \times \mathrm{e}^{-k_{\mathrm{AB}}\times t}$ in which $\mathrm{nFv}^{\mathrm{STF}}(\sim 2)$ is the maximal STF-induced variable fluorescence in Q_B-nonreducing RCs, and k1 and kAB are rate constants of Y_Z^+ reduction and Q_A^- oxidation, respectively. The equation above illustrates and would allow quantification of the amply documented four periodic (Schreiber and Neubauer 1987; Kolber et al. 1998; Shinkarev 2004) and binary oscillation (Bowes and Crofts 1980; Shinkarev 2004) of the STF-induced variable fluorescence in relation to those of the rate (constants) of Y_Z^+ reduction ($k1$) and Q_A^- oxidation (kAB), respectively. For example, if one assumes $\mathrm{nFv}^{\mathrm{STF}} = 2$ (Vredenberg et al. 2007), $k_{si} = k_1 = 10$, 3, 1, and 30 ms^{-1} for OEC in state $S = S_1$, S_2, S_3 and $S_4(0)$, respectively (Babcock 1987) and kAB oscillating between 4 and 2 ms^{-1} (Bowes and Crofts 1987, Vredenberg et al. 2006) one would get the following oscillating $F(t)$/F0 pattern 0.9, 0.6, 0.2, and 1.6 for a dark-adapted system with 100% $S_1$and no misses and double hits. This pattern with minima at STF number 3, 7, etc. is qualitatively in agreement with experimental results (Shinkarev et al. 1997).

In conclusion, the present results and quantitative analyses indicate that estimation and calculation of the parameter of intersystem connectivity (Strasser 1978; Trissl and Lavergne 1995; Zhu et al. 2005), from the sigmoidicity of the MTF-induced fluorescence induction curve $F(t)$ should be done only at high excitation rate, preferentially with STFs, or at rates below ~ 0.5 ms^{-1} equivalent with a light intensity below ~ 150 µmol m^{-2} s^{-1} of red light (650 nm) with correction for the effect associated with double hits. This is essential to circumvent interference from the sigmoidicity of $F(t)$ responses (Figs. 4 and 5) associated with the interplay between the rate constants of light excitation and donor side quenching release and with a double hit trapping mechanism. Sigmoidicity is quantitatively predicted by the single hit trapping concept (Eq. 3) under conditions at which both rate constants are different by less than one order of magnitude. The decrease in degree of sigmoidicity with decrease in excitation rate (intensity) and the absence of sigmoidicity in laser flash (STF) induced changes in fluorescence emission in spinach chloroplasts would indicate that intersystem exciton transfer is negligible, despite the fact that these preparations like the ones we have used here, show sigmoidicity in MTFs. Our data suggest that PSU connectivity in dark-adapted chloroplasts is substantially less, if not negligible, then commonly concluded from the sigmoidicity of the fluorescence induction curve.

Acknowledgment I thank Jack van Rensen for many discussions and Gustavo Rodrigues for assistance in doing the experiments.

Appendices

A. Derivation of the rFv(t) expression when light excitation rate k_L for fluorescence emission is equal to the rate constant of the release of donor side quenching k_{s_1}

Equation 3 gives the general expression for the normalized variable fluorescence $\mathrm{rFv}(t) = y_2(t)$ upon light excitation at a rate k_L and under control of donor side quenching of which the release occurs with a rate constant k_{s_1}

$$y_2(t) = 1 - \frac{k_{s_1}}{k_{s_1} - k_L}\mathrm{e}^{-k_L t} + \frac{k_L}{k_{s_1} - k_L}\mathrm{e}^{-k_{s_1} t} \tag{11}$$

The equation is not applicable when $k_L = k_{s_1}$. Here I give the derivation for the expression of $y_2(t)$ for this particular condition. After rewriting Eq. 3 and series expansion of the function $\mathrm{e}^{-(k_{s_1}-k_L)t}$ (rows 2 and 3, respectively, in the derivation below) one obtains with substitution $k_L = k_{s_1}$ at the end of the third row:

$$\begin{aligned} y_2(t) &= 1 - \mathrm{e}^{-k_L t} \times \left[1 - \frac{k_L}{(k_{s_1} - k_L)}[\mathrm{e}^{-(k_{s_1}-k_L)t} - 1]\right] \\ &= 1 - \mathrm{e}^{-k_L t} \times \left[1 - \frac{k_L}{(k_{s_1} - k_L)}[1 - (k_{s_1} - k_L)t \right. \\ &\quad \left. + \frac{(k_{s_1} - k_L)^2 t^2}{2} - \{\text{higher order terms}\} - 1]\right] \\ &= 1 - \mathrm{e}^{-k_L t}(1 + k_L t) \end{aligned} \tag{A.1}$$

The plot of this relation is shown as the bold curve in Fig. 2a.

The relative variable fluorescence rFv in relation to the fraction q of ('closed') centers with Q_A^- for the particular case $k_L = k_{s_1}$ is easily obtained after substitution Eq. 4 in Eq. A.1. This gives

$$\mathrm{rFv} = y_2(t) = q - k_L t \times e^{-k_L t} = q + (1-q)\ln(1-q) \tag{A.2}$$

The plot of this rFv versus q relation for $k_L = k_{s_1}$ is shown as the bold curve in Fig. 2b.

B. Is the non-linear relation between rFv and the fraction$q$ of centers with Q_A^- ('closed' RCs) (or between V and B, respectively, in Strasser's terminology) a decisive indicator of energetic connectivity between RCs of PSII?

The answer is no, it is not. This will become clear from a closer look at the experimental procedure with which the fraction q (or B in Strasser's terminology) of (closed) centers with Q_A^- is determined. $B(t)$ is obtained, in the presence of DCMU, by numerical determination of the normalized area S(t) above the rFv(t) curve which gives the $B(t)$ curve. The shape of the rFv(t) versus $B(t)$ plot finally is used as a criterion for a nongrouping- (linear relation with rFv(t) = $B(t)$), or grouping- (hyperbolic relation between rFv(t) and $B(t)$) behavior of the PSII systems. In the latter case the connectivity) of the RCs of PSII is related to the empirically derived grouping parameter p by fitting the experimental rFv versus B relation with the hyperbolic relation

$$\mathrm{rFv}(t) = \frac{B(t)}{[1 + C_{hyp}(1 - B(t))]} \tag{B.1}$$

This relation (Strasser 1978), which is similar to one derived by Joliot and Joliot (1964), simplifies for $C_{hyp} = 0$ (no grouping, or noncooperativity) to a linear relation rFv(t) = $B(t)$. Equation B.1 is identical with Eq. 7 with $B(t) = q(t)$. So far so good.

However, it should be realized that $B(t)$ determined from the area above an experimental rFv curve gives the fraction q^{dsq} of RCs in which the donor side quenching is released. As has been derived (see text and Eqs. 1 and 3) q^{dsq} ($= y_2$) $< q$ ($= 1 - y_0$). The unknown fraction y_1 of RCs with Q_A^- and rFv = 0 (due to quenching by donor side components) cannot be detected by the experimental area determination method; it remains hidden due to its quenched properties. Thus what in these graphic analyses routinely is considered as the rFv versus q relation in fact is the non-linear relation between rFv and q^{dsq} fraction of RCs in which fluorescence quenching is released. Its non-linearity is quantitatively related to the release of donor side fluorescence quenching of which the rate constant becomes apparent as an approximately exponential rise in the tens of μs time range in ultra short STFs (Steffen 2003). Theoretically one would have found (see text) a linear relation between rFv and the fraction of closed centers if (i) the fraction q could have been estimated instead of q^{dsq} and (ii) the effect of other inductors is comparatively small. In general the discrepancy between the outcome of the theoretical and experimental rFv versus q relation (with exclusion of improbable systematic errors in the experimental approach) might be caused by (impact factor is presumed to descend with order):

1. Neglecting fluorescence quenching by redox intermediates at the donor side of PSII (donor side quenching).
2. The fact that the closure of RCs in PSII is a double hit trapping process in which closure occurs via semi-open RCs (with 100% Q_A^-) formed from open centers (100% Q_A) in the first hit, as described in the Three State Trapping Model (TSTM).
3. As yet unknown processes including that associated with (changes in) photo-electric fields.
4. A variable and time dependent excitation rate k_L caused for instance by intersystem energy transfer (connectivity) between PSUs of PSII.
5. A combination of 1–4.

C. On the significance of the rFv versus complementary area (B) relation in the concept of the double hit trapping model (TSTM)

The normalized area $B(t)$ above an experimental rFv curve measured in the presence of DCMU does not bear a *simple* relation to the fraction of closed PSII centers $q(t)$ when the concept of TSTM is adopted. Here it is shown that, within this concept, the rFv versus B relation is non-linear, even under conditions at which k_L is time independent (no connectivity) and the effect of donor side quenching is negligible, for instance at $k_L \ll k_{s_1}$. In that case (see Hiraki et al. 2003; Vredenberg 2004 for illustration of scheme and meaning of subscript numbering) the reaction pattern can be represented by the scheme $y_0 \rightarrow y_2 \rightarrow y_4$ with rate constant k_L for both steps; y_0 (=1), y_2 and y_4 refer to the open (y_0), semi-open(-closed) and closed state of PSII systems with relative fluorescence yields rFv equal to 0, 0.5 and 1, respectively. In this simple form and *assuming a time-independent excitation rate* k_L, the solution of the ODEs for y_0, y_2 and y_4 are identical to those given in Eqs. 1–3 with the proper substitutions of the subscripts for the y-states in Eqs. 2 and 3 and substituting $k_{s_1} = k_L$. This gives (see also Eqs. 3a and A.1]), according to definitions:

$$y_2(t) = k_L t e^{-k_L t} \quad \text{(C.1)}$$

$$y_4(t) = 1 - e^{-k_L t}(1 + k_L t) \quad \text{(C.2)}$$

$$\mathrm{rFv}(t) = 0.5 y_2(t) + y_4(t) = 1 - e^{-k_L t}\left(1 + \frac{k_L t}{2}\right) \quad \text{(C.3)}$$

and

$$B(t) = \frac{\int_0^t [1 - \mathrm{rFv}(t)]\mathrm{d}t}{\int_0^\infty [1 - \mathrm{rFv}]\mathrm{d}t} = 1 - e^{-k_L t}\left(1 + \frac{k_L t}{3}\right) \quad \text{(C.4)}$$

Equations C.3 and C.4 show that rFv is non-linearly related to the area B above rFv under conditions in which donor side quenching and intersystem energy transfer can be excluded. Thus a double hit trapping mechanism like TSTM causes a non-linear relation between the relative variable fluorescence (rFv) and the area above the induction curve in the absence of donor side quenching and of connectivity between PSUs.

References

Anderson JM, Melis A (1983) Localization of different photosystems in separate regions of chloroplast membranes. Proc Natl Acad Sci USA 80:745–749

Babcock G (1987) The photosynthetic evolving process. In: Amesz J (ed) New comprehensive biochemistry, vol 15. Elsevier, Amsterdam, pp 125–158

Belyaeva NT, Paschenko VZ, Renger G, Riznichenko Yu G, Rubin AB (2006) Application of photosystem II model for analysis of fluorescence induction curves in the 100 ns to 10 s time domain after excitation with a saturating light pulse. Biophysics (Translated from Biofizika) 51(6):976–990

Bernhardt K, Trissl H-W (1999) Theories for kinetics and yields of fluorescence and photochemistry: how, if at all, can different models of antenna organization be distinguished experimentally? Biochim Biophys Acta 1409:125–142

Black MT, Brearley TH, Horton P (1986) Heterogeneity in chloroplast photosystem II. Photosynth Res 8:193–207

Bolhar-Nordenkampf HR, Long SP, Baker NR, Öquist G, Schreiber U, Lechner EG (1989) Chlorophyll fluorescence as a probe of the photosynthetic competence of leaves in the field: a review of current instrumentation. Funct Ecol 3:497–514

Bowes JM, Crofts AR (1980) Binary oscillations in the rate of reoxidation of the primary acceptor of Photosystem II. Biochim Biophys Acta 590:373–384

Briantais JM, Vernotte C, Krause GH, Weiss E (1986) Chlorophyll *a* fluorescence of higher plants: chloroplasts and leaves. In: Govindjee Amesz J, Fork DC (eds) Light emission by plants and bacteria. Academic Press, Orlando, pp 539–583

Butler WL (1972) On the primary nature of fluorescence yield changes associated with photosynthesis. Proc Natl Acad Sci USA 69:3420–3422

Chylla RA, Garab G, Whitmarsh J (1987) Evidence for slow turnover in a fraction of photosystem II complexes in thylakoid membranes. Biochim Biophys Acta 894:562–571

Dau H (1994) Molecular mechanisms and quantitative models of variable photosystem II fluorescence. Photochem Photobiol 60:1–23

Duysens LNM, Sweers HE (1963) Mechanisms of the two photochemical reactions in algae as studied by means of fluorescence. In: Japanese Society of Plant Physiologists (ed) Studies on microalgae and photosynthetic bacteria. University of Tokyo Press, Tokyo, pp 353–372

Geacintov NE, Breton J (1987) Energy transfer and fluorescence mechanisms in photosynthetic membranes. CRC Crit Rev Plant Sci 5:1–44

Govindjee (1990) Photosystem II heterogeneity: the acceptor side. Photosynth Res 25:151–160

Govindjee (2004) Chlorophyll a fluorescence: a bit of basics and history. In: Papageorgiou GC, Govindjee (eds) Chlorophyll a fluorescence: a signature of photosynthesis. Springer, Dordrecht, pp 1–42

Govindjee, Papageorgiou G (1971) Chlorophyll fluorescence and photosynthesis: fluorescence transients. Photophysiology 6:1–50

Govindjee, Amesz J, Fork DC (eds) (1986) Light emission by plants and bacteria. Academic Press, Orlando, pp 539–583

Graan T, Ort DR (1986) Detection of oxygen-evolving photosystem II centers inactive in plastoquinone reduction. Biochim Biophys Acta 852:320–330

Groot ML, Pawlowicz NP, van der Wilderen LJGW, Breton J, van Stokkum IHM, van Grondelle R (2005) Initial electron donor and acceptor in isolated Photosystem II reaction centers identified with femtosecond mid-IR spectroscopy. Proc Natl Acad Sci USA 102:13087–13092

Haldimann P, Tsimilli-Michael M (2005) Non-photochemical quenching of chlorophyll a fluorescence by oxidized plastoquinone: new evidences based on modulation of the redox state of the endogenous plastoquinone pool in broken spinach chloroplasts. Biochim Biophys Acta 1706:239–249

Hiraki M, van Rensen JJS, Vredenberg WJ, Wakabayashi K (2003) Characterization of the alterations of the chlorophyll *a* fluorescence induction curve after addition of photosystem II inhibiting herbicides. Photosynth Res 78:35–46

Hiraki M, Vredenberg WJ, van Rensen JJS, Wakabayashi K (2004) A modified fluorometric method to quantify the concentration effect (pI_{50}) of photosystem II-inhibiting herbicides. Pestic Biochem Physiol 80:183–191

Holzwarth AR, Müller MG, Reus M, Nowaczyk M, Sander J, Rögner M (2006) Kinetics and mechanism of electron transfer in intact photosystem II and in the isolated reaction center: Pheophytin is the primary electron acceptor. Proc Natl Acad Sci USA 103:6895–6900

Hsu BD, Lee J-Y (1995) Fluorescence quenching by plastoquinone in an oxygen-evolving photosystem-II-enriched preparation. J Photochem Photobiol 30:57–61

Joliot P, Joliot A (1964) Etude cinetique de la reaction photochimique liberant l'oxygene au cours de la photosynthèse. CR Acad Sci Paris 258:4622–4625

Joliot P, Joliot A (1973) Different types of quenching involved in photosystem II centers. Biochim Biophys Acta 305:302–316

Joliot P, Joliot A (1977) Evidence for a double hit process in photosystem II based on fluorescence studies. Biochim Biophys Acta 462:559–574

Joliot P, Joliot A (2002) Cyclic electron transfer in plant leaf. Proc Natl Acad Sci USA 99(15):10209–10214

Klimov VV, Krasnovskii AA (1981) Participation of pheophytin in the primary processes of electron transfer at the reaction centers of photosystem II. Biophysics 27:186–198

Koblizek M, Kaftanm D, Nedbal L (2001) On the relationship between the non-photochemical quenching of the chlorophyll fluorescence and the photosystem II light harvesting efficiency. A repetitive flash fluorescence study. Photosynth Res 68: 141–152

Kolber Z, Prasil O, Falkowski P (1998) Measurements of variable chlorophyll fluorescence using fast repetition rate technique. I. Defining methodology and experimental protocols. Biochim Biophys Acta 1367:88–106

Kramer DM, DiMarco G, Loreto F (1995) Contribution of plastoquinone quenching to saturation pulse-induced rise of chlorophyll fluorescence in leaves. In: Mathis P (ed) Photosynthesis: from light to biosphere, vol I. Kluwer Academic Publishers, Dordrecht, pp 147–150

Krause GH, Weiss E (1991) Chlorophyll fluorescence and photosynthesis: the basics. Annu Rev Plant Physiol Plant Mol Biol 42: 313–349

Krause GH, Briantais JM, Vernotte C (1982) Photoinduced quenching of chlorophyll fluorescence in intact chloroplasts and algae: resolution into two components. Biochim Biophys Acta 679: 116–124

Kurreck J, Schödel R, Renger G (2000) Investigation of the plastoquinone pool size and fluorescence quenching in thylakoid membranes and Photosystem II (PSII) membrane fragments. Photosynth Res 63:171–182

Lavergne J, Briantais J-M (1996) Photosystem II heterogeneity. In: Ort DR, Yocum CF (eds) Oxygenic photosynthesis: the light reactions. Series advances in photosynthesis. Kluwer Academic Publishers, Dordrecht

Lavergne J, Leci E (1993) Properties of inactive photosystem II centers. Photosynth Res 35:323–343

Lavergne J, Trissl HW (1995) Theory of fluorescence induction in photosystem II: Derivation of analytical expressions in a model including exciton-radical-pair equilibrium and restricted energy transfer between photosynthetic units. Biophys J 68:2474–2492

Lazár D (2006) The polyphasic chlorophyll a fluorescence rise measured under high intensity of exciting light. Funct Plant Biology 33:9–30

Lazár D, Pospisil P (1999) Mathematical simulation of chlorophyll *a* fluorescence rise measured with 3-(3′,4′-dichlorophenyl)-1,1-dimethylurea-treated barley leaves at room and high temperatures. Eur Biophys J 28:468–477

Lazár D, Tomek P, Ilík P, Nauš J (2001) Determination of the antenna heterogeneity of photosystem II by direct simultaneous fitting of several fluorescence rise curves measured with DCMU at different intensities. Photosynth Res 68:247–257

Mauzerall D (1972) Light induced fluorescence changes in Chlorella, and the primary photoreactions for the production of oxygen. Proc Natl Acad Sci USA 69:1358–1362

Melis A, Homann PH (1976) Heterogeneity of photochemical centers in system II of chloroplasts. Photochem Photobiol 23:343–350

Nedbal L, Trtilek M, Kaftan D (1999) Flash fluorescence induction: a novel method to study regulation of photosystem II. J Photochem Photobiol B Biol 48:154–157

Nedbal L, Soukupova J, Kaftan D, Whitmarsh J, Trtilek M (2000) Kinetic imaging of chlorophyll fluorescence using modulated light. Photosynth Res 66:3–12

Papageorgiou GC, Govindjee (eds) (2004) Chlorophyll a fluorescence: a signature of photosynthesis. Springer, Dordrecht, 818 pp. ISBN 1-4020-3217-X

Rappaport F, Béal D, Joliot A, Joliot P (2007) On the advantages of using green light to study fluorescence yield changes in leaves. Biochim Biophys Acata 1767:56–65

Reifarth F, Christen G, Renger G (1997) Fluorometric equipment for monitoring P680+ reduction in PS II preparations and green leaves. Photosynth Res 51:231–241

Renger G, Eckert HJ, Bergmann A, Bernarding J, Liu B, Napiwotzki A, Reifarth F, Eichler HJ (1995) Fluorescence and spectroscopic studies of exciton trapping and electron transfer in photosystem II of higher plants. Aust J Plant Physiol 22: 167–181

Schansker G, Toth SZ, Strasser RJ (2006) Dark recovery of the Chl a fluorescence transient (OJIP) after light adaptation: the qT-component of non-photochemical quenching is related to an activated photosystem I acceptor side. Biochimica et Biophysica Acta 1757:787–797

Schreiber U (1983) Chlorophyll fluorescence yield changes as a tool in plant physiology. The measuring system. Photosynth Res 4: 361–373

Schreiber U (1986) Detection of rapid induction kinetics with a new type of high-frequency modulated chlorophyll fluorometer. Photosynth Res 9:261–272

Schreiber U, Krieger A (1996) Hypothesis: two fundamentally different types of variable chlorophyll fluorescence in vivo. FEBS Lett 397:131–135

Schreiber U, Neubauer C (1987) The polyphasic rise of chlorophyll fluorescence upon onset of strong continuous illumination: II. Partial control by the photosystem II donor side and possible ways of interpretation. Z Naturforsch 42c:1255–1264

Schreiber U, Hormann H, Neubauer C, Klughammer C (1995) Assessment of photosystem II photochemical quantum yield by chlorophyll fluorescence quenching analysis. Aust J Plant Physiol 22:209–220

Shinkarev VP (2004) Photosystem II: oxygen evolution and chlorophyll a fluorescence induced by multiple flashes. In: Papageorgiou GC, Govindjee (eds) Chlorophyll a fluorescence: a signature of photosynthesis. Springer, Dordrecht, pp 197–229

Shinkarev VP, Xu C, Govindjee, Wraight CA (1997) Kinetics of the oxygen evolution step in plants determined from flash-induced chlorophyll a fluorescence. Photosynth Res 51:43–49

Steffen R (2003) Time-resolved spectroscopic investigation pf photosystem II. PhD thesis. Technical University Berlin

Steffen R, Christen G, Renger G (2001) Time-resolved monitoring of flash-induced changes of fluorescence quantum yield and decay of delayed light emission in oxygen-evolving photosynthetic organisms. Biochemistry 40:173–180

Steffen R, Eckert H-J, Kelly AA, Dörmann P, Renger G (2005) Investigations on the reaction pattern of photosystem II in leaves from Arabidopsis thaliana by time-resolved fluorometric analysis. Biochemistry 44(9):3124–3131

Stirbet AD, Govindjee, Strasser BJ, Strasser RJ (1998) Chlorophyll *a* fluorescence induction in higher plants: Modeling and numerical simulation. J Theor Biol 193:131–151

Strasser RJ (1978) The grouping model of plant photosynthesis. In: Akoyunoglou G (ed) Chloroplast development. Elsevier, North Holland, pp 513–524

Strasser RJ, Govindjee (1992) The F_0 and the O-J-I-P fluorescence rise in higher plants and algae. In: Argyroudi-Akoyunoglou JH (ed) Regulation of chloroplast biogenesis. Plenum Press, New York, pp 423–426

Strasser RJ, Srivastava A, Govindjee (1995) Polyphasic chlorophyll a fluorescence transient in plants and cyanobacteria. Photochem Photobiol 61:32–42

Strasser RJ, Tsimilli-Michael M, Srivastava A (2004) Analysis of the fluorescence transient. In: Papageorgiou GC, Govindjee (eds) Chlorophyll a fluorescence: a signature of photosynthesis. Springer, Dordrecht, pp 321–362

Tomek P, Ilík P, Lazár D, Stroch M, Nauš J (2003) On the determination of Q_B-non-reducing photosystem II centers from chlorophyll a fluorescence induction. Plant Sci 164:665–670

Toth SZ, Schansker G, Strasser RJ (2005) In intact leaves, the maximum fluorescence level (F(M)) is independent of the redox state of the plastoquinone pool: a DCMU-inhibition study. Biochim Biophys Acta 708(2):275–282

Trissl H-W (2002) Theory of fluorescence induction: an introduction. http://www.biologie.uni-osnabrueck.de/biophysik/Trissl/teaching/teaching.html

Trissl H-W, Lavergne J (1995) Fluorescence induction from photosystem II: analytical equations for the yields of photochemistry and fluorescence derived from analysis of a model including exciton-radical pair equilibrium and restricted energy transfer between photosynthetic units. Aust J Plant Physiol 22:183–193

Trissl H-W, Gao Y, Wulf K (1993) Theoretical fluorescence induction curves derived from coupled differential equations describing the primary photochemistry of photosystem II by an exciton radical pair equilibrium. Biophys J 64:974–988

Vasil'ev S, Bruce D (1998) Nonphotochemical quenching of excitation energy in photosystem II. A picosecond time-resolved study of the low yield of chlorophyll a fluorescence induced by single-turnover flash in isolated spinach thylakoids. Biochemistry 37:11046–11054

Vermaas WFJ, Renger G, Dohnt G (1984) The reduction of the oxygen-evolving system in chloroplasts by thylakoid components. Biochim Biophys Acta 764:194–202

Vernotte C, Etienne AL, Briantais JM (1979) Quenching of the system II chlorophyll fluorescence by the plastoquinone pool. Biochim Biophys Acta 545:519–527

Vredenberg WJ (2000) A three-state model for energy trapping and chlorophyll fluorescence in photosystem II incorporating radical pair recombination. Biophys J 79:25–38

Vredenberg WJ (2004) System analysis of photoelectrochemical control of chlorophyll fluorescence in terms of trapping models of Photosystem II: a challenging view. In: Papageorgiou GC, Govindjee (eds) Chlorophyll a fluorescence: a signature of photosynthesis. Springer, Dordrecht, pp 133–172

Vredenberg WJ, Duysens LNM (1963) Transfer and trapping of excitation energy from bacteriochlorophyll to a reaction center during bacterial photosynthesis. Nature 197:355–357

Vredenberg WJ, Rodrigues GC, van Rensen JJS (2002) A quantitative analysis of the chlorophyll fluorescence induction in terms of electron transfer rates at donor and acceptor sides of photosystem II. In: Proc. 12th Int. Congress Photosynthesis, Brisbane, 18–23 Aug., 2001 S14-10 on CD

Vredenberg WJ, van Rensen JJS, Rodrigues GC (2005) On the submaximal yield and photo-electric stimulation of chlorophyll a fluorescence in single turnover excitations in plant cells. Bioelectrochemistry 68:83–90

Vredenberg WJ, Kasalicky V, Durchan M, Prasil O (2006) The chlorophyll a fluorescence induction pattern in chloroplasts upon repetitive single turnover excitations: Accumulation and function of Q_B-nonreducing centers. Biochim Biophys Acta 1757: 173–181

Vredenberg WJ, Durchan M, Prasil O (2007) On the chlorophyll fluorescence yield in chloroplasts upon excitation with twin turnover flashes (TTF) and high frequency flash trains. Photosynth Res 93:183–192. doi 10.1007/s11120-007-9150-8

Zhu X-G, Govindjee, Baker NR, deSturler E, Ort D, Long SP (2005) Chlorophyll a fluorescence induction kinetics in leaves predicted from a model describing each discrete step of excitation energy and electron transfer associated with photosystem II. Planta 223:114–133 doi 10.1007/s00425-005-0064-4